Neurobiology of Aging 65 (2018) 132–139

Contents lists available at ScienceDirect

Neurobiology of Aging

journal homepage: www.elsevier.com/locate/neuaging

Isoprenoids and tau pathology in sporadic Alzheimer's disease

Sandra Pelleieux [a], Cynthia Picard [a,b], Louise Lamarre-Théroux [a], Doris Dea [a], Valérie Leduc [a], Youla S. Tsantrizos [c,d], Judes Poirier [a,b,*]

[a] Douglas Mental Health University Institute, McGill University, Montreal, Canada
[b] Center for Studies on the Prevention of Alzheimer's Disease, McGill University, Montreal, Canada
[c] Department of Chemistry, McGill University, Montreal, Canada
[d] Department of Biochemistry, McGill University, Montreal, Quebec, Canada

ARTICLE INFO

Article history:
Received 6 September 2017
Received in revised form 7 December 2017
Accepted 21 January 2018
Available online 2 February 2018

Keywords:
Mevalonate pathway
Isoprenoids
Alzheimer's disease
Tau phosphorylation
Farnesyl pyrophosphate synthase
Geranylgeranyl pyrophosphate synthase

ABSTRACT

The mevalonate pathway has been described to play a key role in Alzheimer's disease (AD) physiopathology. Farnesyl pyrophosphate (FPP) and geranylgeranyl pyrophosphate (GGPP) are nonsterol isoprenoids derived from mevalonate, which serve as precursors to numerous human metabolites. They facilitate protein prenylation; hFPP and hGGPP synthases act as gateway enzymes to the prenylation of the small guanosine triphosphate (GTP) ase proteins such as RhoA and cdc42 that have been shown to facilitate phospho-tau (p-Tau, i.e., protein tau phosphorylated) production in the brain. In this study, a significant positive correlation was observed between the synthases mRNA prevalence and disease status (FPPS, $p < 0.001$, n = 123; GGPPS, $p < 0.001$, n = 122). The levels of mRNA for hFPPS and hGGPPS were found to significantly correlate with the amount of p-Tau protein levels ($p < 0.05$, n = 34) and neurofibrillary tangle density ($p < 0.05$, n = 39) in the frontal cortex. Interestingly, high levels of hFPPS and hGGPPS mRNA prevalence are associated with earlier age of onset in AD ($p < 0.05$, n = 58). Together, these results suggest that accumulation of p-Tau in the AD brain is related, at least in part, to increased levels of neuronal isoprenoids.

1. Introduction

Alzheimer's disease (AD) is the most common cause of dementia, with an estimated prevalence of 47 million cases worldwide (World Alzheimer report 2016). The incidence of the disease rises dramatically with age. AD is a complex multifactorial disorder that involves numerous susceptibility genes, but the exact pathogenesis and biochemical basis of AD is not well understood. In recent years, altered lipid metabolism has been extensively implicated in late-onset AD (LOAD) pathogenesis (Reitz, 2013). In addition to the *APOE* gene, many of the LOAD susceptibility loci identified through genome wide association (GWA) studies and meta-analyses are also involved in lipid metabolism (Beecham et al., 2014; Lambert et al., 2013). For example, genes such as *APOE* and *CLU* (apoJ) regulate extracellular cholesterol transport; *BIN1*, *SORL1*, and *PICALM* mediate cholesterol-rich lipoprotein (HDL) internalization, whereas *ABCG1* and *ABCA7* act as chaperone proteins involved in intracellular and transmembrane cholesterol transport (Leduc et al., 2010; Poirier et al., 2014; Taira et al., 2001; Abe-Dohmae et al., 2004).

Recently, the mevalonate metabolic pathway has generated renewed attention in AD (Cole and Vassar, 2006; Hooff et al., 2010; Mohamed et al., 2015), particularly through the 3-hydroxy-3-methyl-glutaryl-coenzyme A reductase (HMGCoA-R) inhibition by statins, a family of drugs widely used to lower circulating cholesterol levels. Previous use of HMGCoA-R inhibitors (statins) by deceased cognitively normal elderly subjects from a population-based epidemiological study was shown to correlate with a significant reduction (−66%) in brain neurofibrillary tangle (NFT) density when compared with age-matched nonusers (Li et al., 2007). However, the use of statins failed to show any additional benefit on markers of cardiovascular pathology or on amyloid plaque density at autopsy. Complementary evidence obtained from humans indicated that the use of statins by AD dementia patients was associated with significant reductions in cerebrospinal fluid p-Tau protein (Riekse et al., 2006), but not with β-amyloid 40 ($A\beta_{40}$) or β-amyloid 42 ($A\beta_{42}$) concentration, the classical components of senile plaques.

Furthermore, 3 large retrospective epidemiological studies examined the putative protective effects of statins in LOAD and showed a marked risk reduction in users of the cholesterol-lowering

* Corresponding author at: Research Program in Aging, Cognition and Alzheimer's Disease, Douglas Mental Health University Institute, 6875 Lasalle, Verdun, Quebec, Canada H4H 1R3. Tel.: +1 514-761-6131x6153; fax: +1 514-888-4094.
E-mail address: judes.poirier@mcgill.ca (J. Poirier).

0197-4580/$ – see front matter © 2018 Elsevier Inc. All rights reserved.
https://doi.org/10.1016/j.neurobiolaging.2018.01.012

drugs (Bettermann et al., 2012; Jick et al., 2000; Wolozin et al., 2007). Wolozin et al. (2007) used a US Veterans Administration databank to follow prospectively 4.5 million veterans aged 65 years and older, showing that only simvastatin significantly reduced incidence of AD, with a hazard ratio of 0.5 (i.e., a 50% reduction in risk, $p < 0.0001$), whereas other statins (atorvastatin and lovastatin) failed to show any "beneficial" effect. However, the cross-sectional nature of these studies raised concerns based on the potential for unanticipated biases including confounding by indication. Six-month multicenter treatment trials of simvastatin and atorvastatin in subjects with mild-to-moderate AD dementia failed to show slower progression of symptoms (Feldman et al., 2010; Sano et al., 2011). The latter trials initially raised doubts about the utility of statins in the treatment of AD until more recent prospective epidemiological findings reported robust protective effects with simvastatin (Bettermann et al., 2012; Haag et al., 2009), consistent with the notion that in vivo inhibition of HMGCoA-R enzymatic activity in the brain for many years before the onset of AD symptoms may be effective in decelerating the progression of this disease.

HMGCoA-R is the first and rate-limiting enzyme of the mevalonate pathway that comprises successive enzymatic reactions that convert acetyl-CoA into different final sterol, isoprenoid, and other metabolites. The human farnesyl pyrophosphate synthase (hFPPS) is the key enzyme that regulates both cholesterol and isoprenoid biosynthesis, such as farnesyl pyrophosphate (FPP) and geranylgeranyl pyrophosphate (GGPP); the biosynthesis of the latter is catalyzed by the downstream enzyme human geranylgeranyl pyrophosphate synthase (hGGPPS) as summarized in Fig. 1.

Marked reduction in the brain isoprenoid levels of FPP and GGPP in C57BL/6J mice chronically treated with simvastatin for 21 days has been reported (Eckert et al., 2009). In a pilot experiment, Eckert et al. (2009) also showed that FPP and GGPP levels are significantly increased in the frontal cortex of AD patients, but not cholesterol levels or HMGCoA-R gene expression. Although FPP and GGPP are key metabolites derived from the mevalonate pathway, unlike cholesterol, there is little information on their abundance and regulation in the human brain.

An age-related increase of FPP and GGPP levels has been reported in the brain of mice (Hooff et al., 2012), as well as overexpression of FPP synthase (FPPS) and geranylgeranyl pyrophosphate synthase (GGPPS) mRNA levels; high levels of FPP and GGPP in brain tissue are believed to play a key role in neurodegeneration (Eckert et al., 2009). In aged mouse brains, significant higher level of GGPP might be explained by impairment of geranylgeranyl transferase–I (GGTase-I) gene expression and activity (Afshordel et al., 2014). hFPPS and hGGPPS are essential for post-translational prenylation and activation of all guanosine triphosphate (GTP) ases that play an essential role in a plethora of cellular functions, including cell signaling (Nguyen et al., 2009), proliferation, and synaptic plasticity (Hottman and Li, 2014). Farnesylated proteins include members of the Ras super family of GTPases (Kho et al., 2004), and the geranylated GTPases include the Rho family of proteins such as Rho A/B/C, Rac-1, and Cdc42 (Fig. 1); the latter protein is responsible for activation of the key kinase, glycogen synthase kinase 3 beta (GSK3-β), which is responsible for tau phosphorylation and consequently implicated in the formation of NFTs, a hallmark of AD pathophysiology.

The present study aims to examine the relationships between the biosynthesis of isoprenoids and tau pathology in the central nervous system (CNS) of AD subjects. Prevalence of mRNA levels for hFPPS and hGGPPS has been contrasted with different biomarkers

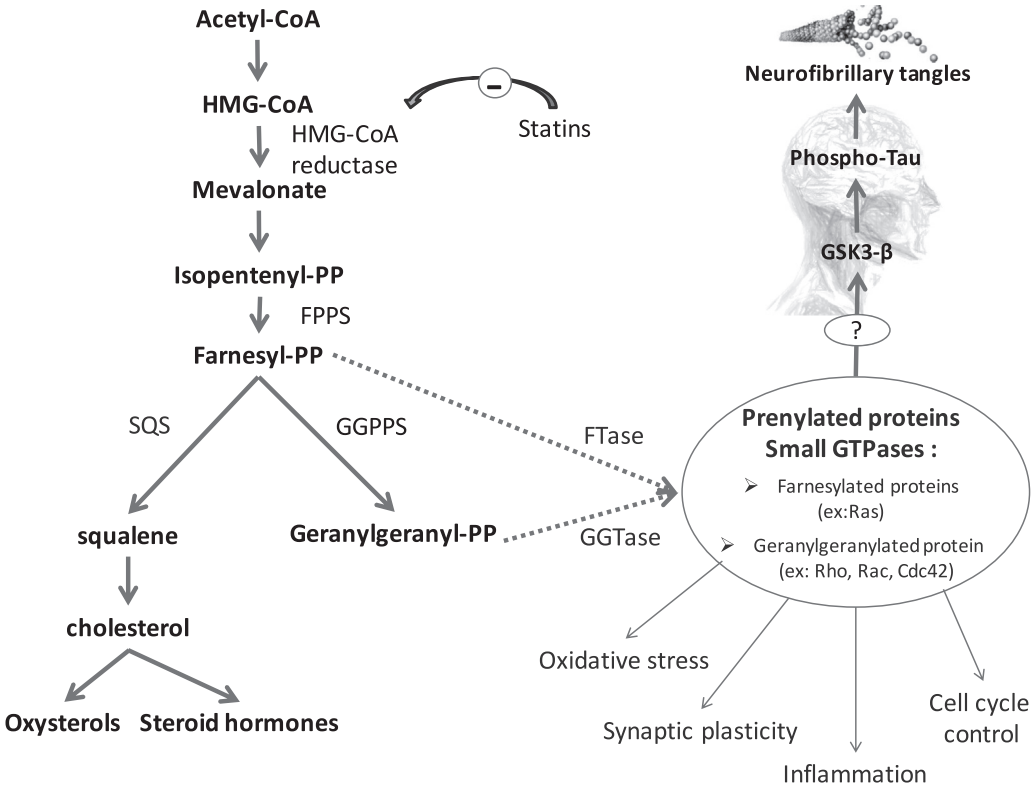

Fig. 1. Schematic representation of pathways associated with the biological role of human FPPS, GGPPS, and tau protein physiopathology identified in Alzheimer's disease and other tau-related diseases. Abbreviations: Acetyl-CoA, acetyl-coenzyme A; FPPS, farnesyl pyrophosphate synthase; FTase, farnesyl transferase; GGPPS, geranylgeranyl pyrophosphate synthase; GGTase, geranylgeranyl transferase; GSK3-β, glycogen synthase kinase 3 beta; HMGCoA-R, 3-hydroxy-3-methyl-glutaryl-coenzyme A reductase; -PP, pyrophosphate; Phospho-Tau, protein tau phosphorylated; SQS, squalene synthase.

Table 1
Demographic characteristics of the studied cohort

Description	Overall	Control	Alzheimer
Number of subjects, *n*	151	55	96
Gender, *n* (%)			
Female	74 (49%)	24 (44%)	50 (52%)
Male	77 (51%)	31 (56%)	46 (48%)
APOE-ε4 carriers**	70 (47%)	12 (21%)	58 (61%)
Age of death (mean ± SD, y)*	78.5 ± 8.7	75.9 ± 10.7	79.9 ± 6.9

NOTE. Statistically significant difference between the controls and Alzheimer's disease groups: $^{*}p < 0.05$ and $^{**}p < 0.01$.
Key: APOE-ε4, apolipoprotein E4 variant; SD, standard deviation.

involved in the mevalonate pathway and in tau pathology in cortical areas in healthy controls and AD individuals.

2. Materials and methods

2.1. Human brain samples

All tissues from the frontal cortex and cerebellum were obtained from the Douglas-Bell Canada Brain Bank, Montreal, Canada. Patients' demographic characteristics are summarized in Tables 1 and 2. Definite diagnosis of AD was based on histopathological confirmation of AD according to NINCDS-ADRDA criteria (Khachaturian, 1985), whereas controls had to be free of neurological or psychiatric diseases and of brain structural lesions (tangle and plaque indices reading $<20/mm^2$ and $<10/mm^2$, respectively). *APOE* genotype distribution is similar to previously reported prevalence for Eastern Canadians with a strong and significant enrichment of the APOE-ε4 allele in autopsied-confirmed AD cases. All procedures were approved by the institutional ethics committee, and all the patients, or his or her legal tutor, signed an informed consent form. Individual postmortem delays did not affect FPP or GGPP levels in tissues nor mRNA prevalence for hFPPS or hGGPPS (data not shown). Postmortem delays were 28 ± 18 hours for controls and 21 ± 13 hours for AD patients.

2.2. Tissue preparation

One hundred milligrams of tissue was homogenized with 1 mL of 100 mM Tris buffer (pH 8.0) containing 10 μL Halt phosphatase inhibitor cocktail and 100 μL PhosSTOP phosphatase inhibitor cocktail by using the Omni Bead Ruptor 24 at 5.65 ms^{-1}, 2 × 30 seconds. The homogenate was centrifuged 5 minutes at 1400 rpm, 4 °C. The supernatant was immediately stored at −80 °C. Samples were again centrifuged 5 minutes at 1400 rpm, 4 °C, before each analysis.

The total protein concentration was estimated using a bicinchoninic acid protein assay kit (Pierce, USA) according to the manufacturer's instructions.

2.3. GSK3-β and HMGCoA-R quantification

Enzyme-linked immunosorbent assay analyses were performed using commercial sandwich enzymes immunoassay kits KHO0451, Invitrogen, for the total GSK3-β protein detection and quantification according to the manufacturer's instructions, and MyBioSource (#MBS742031; CA, USA), for the HMGCoA-R protein levels following the protocol previously described for brain tissues (Leduc et al., 2016) using a Synergy H1 microplate reader (BioTek, VT, USA).

2.4. Phospho-tau quantification and determination of NFT counts

Phospho-tau quantification was assessed in brain homogenates using INNO-BIA AlzBio3 assay (Innogenetics) on a Luminex Bio-Rad apparatus as per the manufacturer's instruction. NFT densities were determined in the frontal cortex as previously described (Leduc et al., 2009) and were consistent with the criteria used in the classification of Khachaturian (Khachaturian, 1985).

2.5. Brain FPP and GGPP levels

Brain sample homogenates (100 μL) were added to 2.5 μL of thymolphthalein monophosphate (1000 ng) as an internal standard (IS) (Su Hyeon Lee et al., 2011) and 300 μL acetonitrile with 2% acid formic and mixed 30 seconds. The mixture was centrifuged 10 minutes at 1400 rpm, 4 °C. Extraction was performed using a solid phase extraction column Strata-XL-AW 100 μm Polymeric Weak Anion (8B-S051 UBJ; Phenomenex) by adding 1 mL methanol following by 1 mL Milli-Q water. Then 1 mL homogenate was spiked with 600 μL water followed by 1 mL of 25 mM ammonium acetate (pH 7) and finally 1 mL methanol. Elution was performed by adding 3 × 500 μL of 5% NH_4OH in methanol. An evaporation step was performed using a Labconco evaporator. Residues in the evaporated tube were dissolved by adding 200 μL of 1% NH_4OH in methanol and finally 5 μL was injected for the liquid chromatography tandem-mass spectrometry (LC-MS-MS) analysis.

LC-MS/MS analysis was performed with the Agilent 1200 Series HPLC System coupled to an AB 3200 QTRAP mass spectrometer. All pyrophosphates were separated using a Luna 3 μm C18 100 Å, LC Column (50 mm × 3 mm; Phenomenex) at 0.7 mL/min. The mobile phases used were A (20 mM ammonium bicarbonate and 0.2% triethylamine in water) and B (0.1% triethylamine in acetonitrile), which were controlled as follows: 0–4 minutes at 0% B; 4–7 minutes at 60%–100% B; 7–7.5 minutes at 100% B;

Table 2
Group of samples available for each subanalysis

Subgroup of patients	Mean PMD (h)	Mean age of onset (y)	Mean age at death (y)	Gender (%)		APOE4 (%)
				M	F	
mRNA FPPS (n = 123)	24	74	79	52	48	48
mRNA GGPPS (n = 122)	24	73	79	51	49	47
FPP (n = 48)	24	77	80	52	48	52
GGPP (n = 107)	25	75	80	50	50	50
mRNA SREBF2 (n = 71)	26	76	82	52	48	46
HMGCoA-R (n = 42)	24	74	76	55	45	45
Cholesterol (n = 61)	21	71	75	52	48	56
Number of tangles (n = 57)	24	76	82	46	54	51
p-Tau (n = 36)	22	75	80	44	56	61
GSK3-β (n = 66)	28	75	81	48	52	48

Key: APOE4, apolipoprotein E4 variant; FPP(S), farnesyl pyrophosphate (synthase); GGPP(S), geranylgeranyl pyrophosphate (synthase); GSK3-β, glycogen synthase kinase 3 beta; HMGCoA-R, 3-hydroxy-3-methyl-glutaryl-coenzyme A reductase; p-Tau, phospho-tau or protein tau phosphorylated; PMD, postmortem delay; SREBF2, sterol regulatory element–binding transcription factor 2.

7.5–8 minutes at 100%–0% B, and 8–10 minutes at 0% B. The gradient was then returned to the initial conditions (0% B) and held for 2 minutes before next sample was run. All pyrophosphates were detected in negative ionization. Multiple reaction monitoring parameters are summarized in Table 3. The MS-MS parameters were optimized via infusion of FPP, GGPP, and thymolphthalein monophosphate (IS) solutions prepared in methanol at a flow rate of 10 μL/min with a syringe pump Hamilton 1750TTL 500 μL (4022184). The mass spectrometer was operated under the following optimized conditions: a curtain gas (CUR) of 25 psi, an ion spray voltage (IS) of −4200 V, a temperature (TEM) of 550 °C, an ion source gas 1 (GS1) of 55 psi, and GS2 of 60 psi.

2.6. Cortical cholesterol

Cortical free-cholesterol levels were assessed with HPLC Varian column Microsorb-MW (100-5 C8 250 X 4.6 mm X) using the Prostar detector. For extraction, 50 μL homogenate was added to H_2O:MeOH:$ChCl_3$ (3:4:8) mix and centrifuged 10 minutes at 2000 rpm, 4 °C. The upper phase was reserved to perform DNA dosage. Eighty microliters of H_2O was added to the lower phase mix and centrifuged 10 minutes at 2000 rpm, 4 °C. An evaporation step was performed on the lower phase using a Labconco evaporator. Residues in the evaporated tube were dissolved by adding 400 μL of isopropanol:chloroform (1:1 [v:v]), and finally 50 μL was injected for the LC-MS-MS analysis. Hepta (4 μg/μL) was used as an IS, and 25 μL was added to each sample to obtain a final concentration of 100 μg. DNA dosage was performed with Quant-IT Picogreen dsDNA reagent kits (# P7589).

2.7. Brain FPPS, GGPPS, and SREBF2 mRNA prevalence

RNA was extracted from human brain samples using the Maxwell 16 Tissue LEV Total RNA Purification Kit (Promega, WI, USA) on the Maxwell 16 LEV Instrument (Promega). The purity and integrity of all RNA samples was estimated using the ratio of absorbance values at 260 nm and 280 nm. Random samples were also assessed for RNA integrity number with the Agilent 2100 Bioanalyzer. Complementary DNA (cDNA) was obtained by reverse transcription using the MultiGene Thermal Cycler (Labnet International, Inc.) with SuperScript VILO Master Mix (Invitrogen, Carlsbad, CA, USA). hSREBF2, hGGPPS, and hFPPS gene expression levels were quantified by real-time PCR using the QuantStudio 12K Flex system (Applied Biosystems, Waltham, MA, USA), 10 ng of cDNA, and TaqMan Gene Expression Assay Kit (hSREBF2: #Hs01081784_m1, hGGPPS: #Hs00191442_m1, and hFPPS: #Hs01560316-g1). Hypoxanthine phosphoribosyltransferase (HPRT) was used for calibration (hHPRT #4326321.E), and relative gene expression levels were determined using the comparative Ct method. Of note, HPRT was chosen as the best housekeeping gene among 5 other genes (PPIA, UBE2D2, CDKN1B, ACTB, and GAPDH), as calculated using BestKeeper (Pfaffl et al., 2004) and NormFinder (Andersen et al., 2004).

Table 3
LC-MS-MS parameters

Pyrophosphate	Molecular weight	Q1 Mass (m/z)	Q3 Mass (m/z)	Declustering potential (V)	Entrance potential (V)
FPP	382.3	381.0	79.0	−40.0	−40.0
GGPP	450.4	449.2	79.0	−40.0	−44.0
TMP (IS)	554.5	509.2	79.0	−45.0	−38.0

Key: FPP, farnesyl pyrophosphate; GGPP, geranylgeranyl pyrophosphate; TMP, thymolphthalein monophosphate; IS, internal standard; Q1, precursor ion; Q3, product ion; m/z, mass-to-charge ratio.

2.8. Statistics

All statistics were carried out using SPSS program. As expected, given their high interindividual variability, most of the data produced in this article were non-normally distributed (assessed via Kolmogorov-Smirnov, Shapiro-Wilk tests, and visual inspection of Q-Q plots). Nonparametric tests were used to assess the relationship between the variables by calculation of the Spearman's rank correlation coefficient. All data are expressed as mean value ± standard error of the mean (SEM) unless stated otherwise.

3. Results

3.1. Relationship between brain isoprenoids, key enzymes of the mevalonate pathway, and tau pathology

We used Spearman correlations to investigate whether hFPPS and hGGPPS mRNA prevalence in the human frontal cortex is associated with specific biomarkers involved in the mevalonate pathway and/or with tau pathology. Table 4 provides a summary of the results. The cerebellum was used as a positive, pathology-free, control brain region in these studies.

Table 4
Statistical relation between brain isoprenoids FPP and GGPP, in the human CxF, as a function of APOE4 genotype, gender, and biological markers involved in the mevalonate pathway and tau pathology

Description		RQ FPPS CxF	RQ GGPPS CxF
	APOE4 genotype		
	Correlation coefficient	0.204	0.204
	p-value	**0.024**	**0.025**
	n	122	121
	Gender		
	Correlation coefficient	−0.156	−0.210
	p-value	0.086	**0.021**
	n	122	121
Mevalonate pathway	mRNA SREBF2 CxF (RQ)		
	Correlation coefficient	0.284	0.404
	p-value	**0.017**[a]	**0.001**[a]
	n	70	69
	HMG-CoA-R CxF (ng/mg prot)		
	Correlation coefficient	0.356	0.293
	p-value	**0.039**[a]	0.093
	n	34	34
	Cholesterol CxF (μg/μDNA)		
	Correlation coefficient	0.059	0.055
	p-value	0.670	0.695
	n	54	54
Tau pathology	Number of tangles CxF		
	Correlation coefficient	0.546	0.347
	p-value	**0.000**[a]	**0.030**[a]
	n	40	39
	p-Tau CxF (pg/mg prot)		
	Correlation coefficient	0.469	0.393
	p-value	**0.004**	**0.021**[a]
	n	35	34
	GSK3-β CxF (ng/mg prot)		
	Correlation coefficient	−0.456	−0.460
	p-value	**0.000**[a]	**0.000**[a]
	N	63	62

Bold values: significant association ($p < 0.05$) before controlling for APOE4 genotype and gender.
Key: AD, Alzheimer's disease; CxF, frontal cortex; GGPP(S), geranylgeranyl pyrophosphate (synthase); FPP(S), farnesyl pyrophosphate (synthase); prot, proteins; GSK3-β, glycogen synthase kinase 3 beta; p-Tau, phospho-tau or protein tau phosphorylated; HMGCoA-R, 3-hydroxy-3-methyl-glutaryl-coenzyme A reductase; SREBF2, sterol regulatory element–binding transcription factor 2; RQ, relative quantification of mRNA; n, number of measurements; *p*-value, Spearman coefficient at risk $\alpha = 0.05$.
[a] Significant after controlling for APOE4 genotype and gender.

3.1.1. hFPPS/hGGPPS mRNA prevalence and HMGCoA-R

In the frontal cortex, a positive significant association was found between mRNA prevalence of SREBF2 and hFPPS ($p = 0.017$, n = 70) or hGGPPS ($p = 0.001$, n = 69). SREBF2 is a well-known transcription factor regulating hFPPS expression (Sato, 2009). A positive association was found between mRNA prevalence of hFPPS and hGGPPS and the protein levels of HMGCoA-R ($p = 0.039$, n = 34 for hFPPS and trend only; $p = 0.093$, n = 34 for hGGPPS) but not with cortical free-cholesterol levels.

3.1.2. mRNA of hFPPS/hGGPPS and tau pathology

In the frontal cortex, a positive correlation was found between p-Tau levels and both hFPPS and hGGPPS mRNA prevalence ($p = 0.004$, n = 35, and $p = 0.021$, n = 34, respectively). Moreover, a positive correlation was also found between the NFT density and hFPPS ($p < 0.000$, n = 40) and hGGPPS ($p = 0.030$, n = 39) mRNA prevalence. Conversely, a significant negative correlation was found between total GSK3-β protein levels and the mRNA prevalence of both synthases ($p < 0.0001$ for both hFPPS, n = 63, and hGGPPS, n = 62).

3.2. Relationship between isoprenoid levels in the frontal cortex and the age of onset of AD

Fig. 2 illustrates the relationship between mRNA levels of the cortical synthases as a function of the age of onset of AD, whereas the inserts show the relation between FPP/GGPP and the age of onset in AD. A significant negative correlation was observed between age of onset and hFPPS ($p = 0.004$, n = 59, Fig. 2A) and hGGPPS ($p = 0.021$, n = 58, Fig. 2B) transcripts prevalence, suggesting that the higher the expression, the earlier the onset of the disease. For FPP and GGPP precursor compounds measured by LC-MS-MS, the relation failed to reach significance, yet a similar trend was observed where the lower levels of isoprenoids are associated with a delayed age of onset.

3.3. Quantification of isoprenoids in human brain tissues in controls and AD subjects

In the cerebellum, which was used here as a control brain region with little or no pathology for AD, analyses did not reveal any correlation between the disease status and transcripts prevalence for hFPPS ($p = 0.293$, n = 47, Fig. 3A) or for FPP ($p = 0.721$, n = 53, Fig. 3C) or for GGPP levels ($p = 0.133$, n = 108, Fig. 3D). There is however a modest but significant increase in hGGPPS mRNA prevalence levels ($p = 0.014$, n = 47, Fig. 3B) in AD tissue as compared to controls.

In contrast, in the frontal cortex, an important significant increase of 64% (Fig. 3A) and 81% (Fig. 3B) was observed, respectively, for hFPPS ($p < 0.0001$, n = 123) and hGGPPS ($p < 0.0001$, n = 122) mRNA prevalence in AD tissues as compared to controls.

The significant upregulation of the mRNA prevalence of these enzymes is associated with higher levels of isoprenoids in the cortical area. Indeed, GGPP concentrations are significantly increased in AD brains (+47%, $p = 0.005$, n = 107, Fig. 3D), whereas FPP levels tend to follow as same trend (+25%, $p = 0.08$, n = 48, Fig. 3C). FPP measures were performed near lower detection limit of the LC-MS/MS; explaining the 50% reduction in sample size.

4. Discussion

Currently, there is little information pertaining to regulation of isoprenoids in the human brain, mainly due to analytical difficulties in reliably measuring regional FPP and GGPP levels. Recently, we optimized a novel method using LC-MS-MS to circumvent these issues. Results indicate that GGPP levels are significantly higher than FPP levels (2.5 fold, Fig. 3), consistent with preliminary reports in mouse brains and autopsied human AD brains (Eckert et al., 2009; Hooff et al., 2008; Tong et al., 2008). Cortical GGPP levels are significantly higher in brain tissue of AD patients (+47%, $p < 0.01$) as opposed to FPP levels (+25%; $p = 0.08$). Transcript prevalence for hFPPS (n = 75) and hGGPPS (n = 74) are markedly increased in AD patients as compared to age-matched controls (n = 48), that is, +64% for hFPPS ($p < 0.001$) and +81% for hGGPPS ($p < 0.001$) (Fig. 3). These results are consistent with a pilot study in 13 males where the levels of FPP (+36%) and GGPP (+56%) were reported to be increased in whole-brain tissues from AD subjects (Eckert et al., 2009). One explanation for elevated GGPP levels in aged mouse brains comes from decrease in GGTase-I expression, protein levels, and activity (Afshordel et al., 2014).

High levels of cortical isoprenoids and synthases gene expression correlated with an earlier age of onset in our cohort of AD subjects (Fig. 2). For example, AD subjects with an age of onset below 70 years display mRNA prevalence of 2.6 ± 1.6 (hFPPS) and 2.5 ± 1 (hGGPPS), whereas subjects with onset above 80 years of age exhibit mRNA prevalence of 1.6 ± 0.9 (hFPPS) and 1.3 ± 0.9 (hGGPPS), almost a 50% reduction. These marked changes in mRNA levels (and presumably expression levels of the synthase enzymes) are bound to affect the downstream isoprenoid cascade and the different kinases involved in AD pathophysiology, such as the ones involved in p-Tau production and Aβ metabolism.

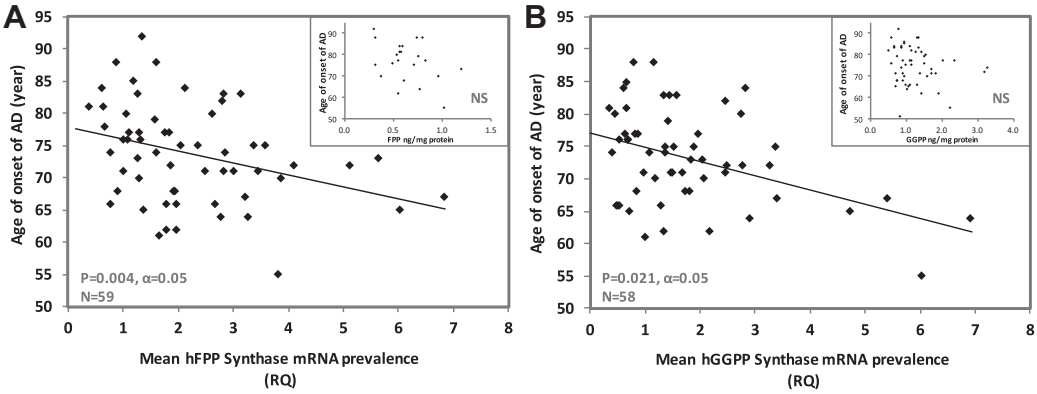

Fig. 2. mRNA levels of hFPPS (A) and hGGPPS (B) measured by RT-qPCR, and FPP (A) and GGPP (B) measured by LC-MS-MS in the frontal cortex as a function of the age of onset of AD. Abbreviations: AD, Alzheimer's disease; FPP, farnesyl pyrophosphate; GGPP, geranylgeranyl pyrophosphate; NS, not significant; RQ, relative quantification.

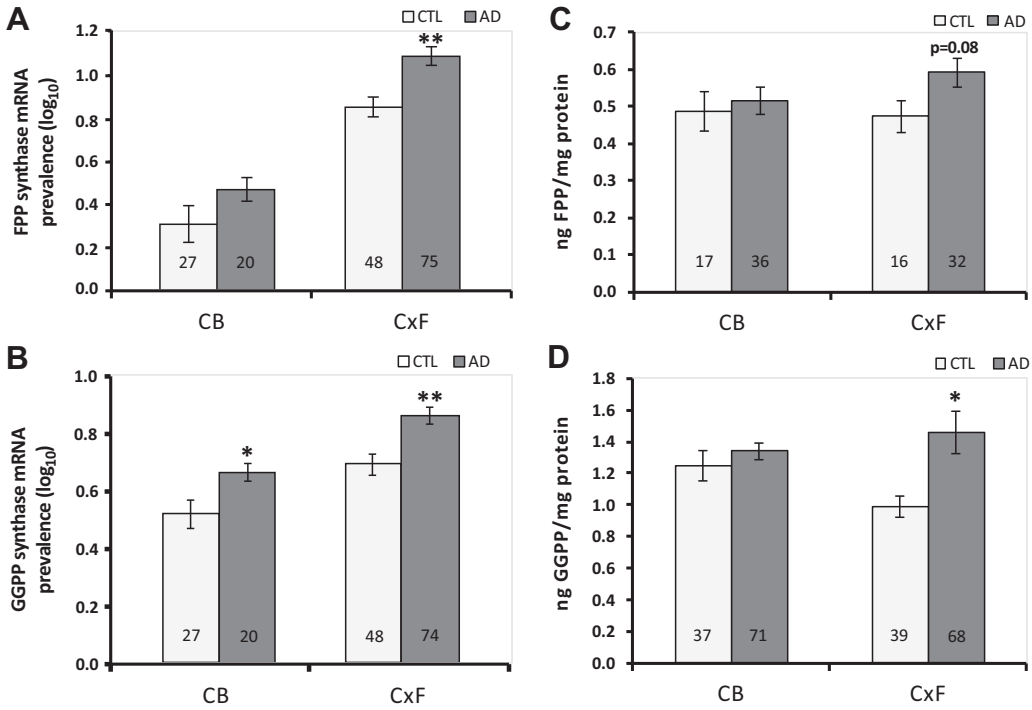

Fig. 3. Cerebellar and cortical, mean ± SEM, mRNA levels of hFPPS (A) hGGPPS (B) measured by RT-qPCR, and FPP (C) and GGPP (D) measured by LC-MS-MS in human AD and control brains. * Correlation is significant at the 0.05 level, and ** correlation is significant at the 0.01 level. Abbreviations: AD, Alzheimer's disease; CB, cerebellum; CTL, control; CxF, frontal cortex; FPP, farnesyl pyrophosphate; GGPP, geranylgeranyl pyrophosphate; prot, proteins; RQ, relative quantification; SEM, standard error of the mean.

At the start of the cascade, HMGCoA-R is the first and rate-limiting enzyme involved in the mevalonate pathway that leads to the synthesis of both cholesterol and isoprenoids in the brain (Fig. 1). Human FPPS is responsible for the biosynthesis of FPP, which is a precursor of both GGPP and cholesterol (Fig. 1). In the human frontal cortex, hFPPS and hGGPPS mRNA prevalence significantly correlates with SREBF2 mRNA prevalence ($p < 0.02$ and $p < 0.001$, respectively), a well-known transcription factor that regulates HMGCoA-R and hFPPS gene expressions in the CNS (Hooff et al., 2010; Sato, 2009). Furthermore, transcript prevalence for hFPPS and hGGPPS was shown to positively correlate with an increase in HMGCoA-R proteins levels in cortical areas, but not with total tissues cholesterol levels (Table 4), suggesting that isoprenoids involvement in the neurodegenerative process behind AD is actually independent from local cholesterol production (Eckert et al., 2009; Wood et al., 2014).

Both FPP and GGPP are required for prenylation of small GTPases necessary to their activation and insertion into cell. Majority of small Rho-GTPases, such as Rac1, RhoA, and Cdc42, are prenylated by GGPP involving GGTase-I, which catalyzes the covalent attachment of GGPP to the enzyme. FPP mainly prenylates Ras proteins through actions of farnesyl transferase, but when farnesyl transferase is inhibited, FPP becomes a substrate for GGTase-I (Downward, 2003; Wood et al., 2014; Roskoski, 2003). Experimental evidence suggests that isoprenylated GTPases are directly involved in AD pathogenesis (Huesa et al., 2010; Ostrowski et al., 2007; Scheper et al., 2007; Wang et al., 2009).

It has been proposed that isoprenoids can modulate p-Tau production in the human brain via the metabolic cascade FPP→GGPP→GTPases→GSK3-β→p-Tau (Ohm et al., 2003; Park et al., 2014; Sayas et al., 1999). Using a cellular model of tauopathy, pitavastatin was shown to decrease tau levels via a coordinated reduction of isoprenoids synthesis and inactivation of Rho (Hamano et al., 2012). Pitavastatin-mediated reductions of total and p-Tau levels can be reversed by the addition of mevalonate or GGPP. It also restores the activity of GSK3-β (Hamano et al., 2012). GSK3, cdk5, and MAPK kinases have been shown to phosphorylate tau protein on serine and threonine residues (Hanger et al., 2009; Kremer et al., 2011).

An excess of phosphorylation of tau protein leads to NFT formation, a landmark pathological feature of AD (Brion et al., 1986; Grundke-Iqbal et al., 1986). We found a positive significant association between the cortical tangle density, p-Tau levels, and mRNA prevalence for hFPPS and hGGPPS (Table 4); consistent with the notion that enhanced isoprenoids production affects tau metabolism via isoprenylation of key regulatory kinases involved in tau pathology. GSK3-β, the most dominant tau kinase (Takashima, 2006), is present in neurons and is normally found on the post-synaptic density in dendritic spines in mouse brains (Perez-Costas et al., 2010). We report here a strong negative correlation between the kinase levels and mRNA prevalence of hFPPS and hGGPPS (Table 4) in the cortex in AD. It is unclear at this time whether the reduction is entirely due to the isoprenoids alterations or local neuronal loss. Moreover, GSK3-β requires a priming phosphorylation of these residues by other tau kinases. We tried without success to measure phosphorylated GSK3-β protein levels (at residue 9) in our autopsied cortical and cerebellar human tissues using a highly specific and sensitive enzyme-linked immunosorbent assay, but all measured data were below the detection limit (data not shown).

Those results suggest that the extent of AD tau pathology could be modulated by a dysregulation of the isoprenoid pathway, indirectly affecting tau metabolism. It is tempting to speculate that cerebrospinal fluid–isoprenoid levels of FPP and GGPP could be used as novel surrogate biomarkers of progression for the pre-symptomatic and early stages of AD. However, we need further evidence that these alterations actually predict the conversion from normal or prodromal AD to formal AD status. Because FPP and GGPP

dysregulations have been proposed to be involved in disease and conditions as diverse as osteoporosis (Mo et al., 2012), cancer (Wiemer et al., 2009), cardiovascular disease (Liao and Laufs, 2005), and premature and normal aging (Hooff et al., 2012), AD patients, but not exclusively, could benefit from the development of new specific and potent isoprenoid inhibitors.

5. Conclusion

Taken together, these results suggest that, in human brain, homeostasis of mevalonate pathway and, especially, intracellular levels of isoprenoids are specifically involved in AD tau pathology and are independent of cholesterol homeostasis. These results also showed that AD patients present higher levels of FPP, GGPP, and related enzymes in the frontal cortex, and that the higher levels of isoprenoids in the brain are correlated with an earlier age of onset of AD.

Disclosure statement

The authors report no conflicts of interest.

Acknowledgements

This work was funded by J.L. Levesque (Judes Poirier), Alcan Rio Tinto (Judes Poirier), and the Canadian Institute on Health Research (Judes Poirier and Youla S. Tsantrizos).

References

Abe-Dohmae, S., Ikeda, Y., Matsuo, M., Hayashi, M., Okuhira, K., Ueda, K., Yokoyama, S., 2004. Human ABCA7 supports apolipoprotein-mediated release of cellular cholesterol and phospholipid to generate high density lipoprotein. J. Biol. Chem. 279, 604–611.

Afshordel, S., Wood, W.G., Igbavboa, U., Muller, W.E., Eckert, G.P., 2014. Impaired geranylgeranyl transferase-I regulation reduces membrane-associated Rho protein levels in aged mouse brain. J. Neurochem. 129, 732–742.

Andersen, C.L., Jensen, J.L., Orntoft, T.F., 2004. Normalization of real-time quantitative reverse transcription-PCR data: a model-based variance estimation approach to identify genes suited for normalization, applied to bladder and colon cancer data sets. Cancer Res. 64, 5245–5250.

Beecham, G.W., Hamilton, K., Naj, A.C., Martin, E.R., Huentelman, M., Myers, A.J., Corneveaux, J.J., Hardy, J., Vonsattel, J.P., Younkin, S.G., Bennett, D.A., De Jager, P.L., Larson, E.B., Crane, P.K., Kamboh, M.I., Kofler, J.K., Mash, D.C., Duque, L., Gilbert, J.R., Gwirtsman, H., Buxbaum, J.D., Kramer, P., Dickson, D.W., Farrer, L.A., Frosch, M.P., Ghetti, B., Haines, J.L., Hyman, B.T., Kukull, W.A., Mayeux, R.P., Pericak-Vance, M.A., Schneider, J.A., Trojanowski, J.Q., Reiman, E.M., Alzheimer's Disease Genetics Consortium (ADGC), Schellenberg, G.D., Montine, T.J., 2014. Genome-wide association meta-analysis of neuropathologic features of Alzheimer's disease and related dementias. PLoS Genet. 10, e1004606.

Bettermann, K., Arnold, A.M., Williamson, J., Rapp, S., Sink, K., Toole, J.F., Carlson, M.C., Yasar, S., Dekosky, S., Burke, G.L., 2012. Statins, risk of dementia, and cognitive function: Secondary analysis of the Ginkgo Evaluation of Memory Study. J. Stroke Cerebrovasc. Dis. 21, 436–444.

Brion, J.P., Flament-Durand, J., Dustin, P., 1986. Alzheimer's disease and tau proteins. Lancet 2, 1098.

Cole, S.L., Vassar, R., 2006. Isoprenoids and Alzheimer's disease: a complex relationship. Neurobiol. Dis. 22, 209–222.

Downward, J., 2003. Targeting RAS signalling pathways in cancer therapy. Nat. Rev. Cancer 3, 11–22.

Eckert, G.P., Hooff, G.P., Strandjord, D.M., Igbavboa, U., Volmer, D.A., Muller, W.E., Wood, W.G., 2009. Regulation of the brain isoprenoids farnesyl- and geranylgeranyl pyrophosphate is altered in male Alzheimer patients. Neurobiol. Dis. 35, 251–257.

Feldman, H.H., Doody, R.S., Kivipelto, M., Sparks, D.L., Waters, D.D., Jones, R.W., Schwam, E., Schindler, R., Hey-Hadavi, J., Demicco, D.A., Breazna, A., 2010. Randomized controlled trial of atorvastatin in mild to moderate Alzheimer disease: LEADe. Neurology 74, 956–964.

Grundke-Iqbal, I., Iqbal, K., Tung, Y.C., Quinlan, M., Wisniewski, H.M., Binder, L.I., 1986. Abnormal phosphorylation of the microtubule-associated protein tau (tau) in Alzheimer cytoskeletal pathology. Proc. Natl. Acad. Sci. U S A. 83, 4913–4917.

Haag, M.D.M., Hofman, A., Koudstaal, P.J., Stricker, B.H.C., Breteler, M.M.B., 2009. Statins are associated with a reduced risk of Alzheimer disease regardless of lipophilicity. The Rotterdam Study. J. Neurol. Neurosurg. Psychiatry 80, 13–17.

Hamano, T., Yen, S.H., Gendron, T., Ko, L.W., Kuriyama, M., 2012. Pitavastatin decreases tau levels via the inactivation of Rho/ROCK. Neurobiol. Aging 33, 2306–2320.

Hanger, D.P., Anderton, B.H., Noble, W., 2009. Tau phosphorylation: the therapeutic challenge for neurodegenerative disease. Trends Mol. Med. 15, 112–119.

Hooff, G.P., Volmer, D.A., Wood, W.G., Muller, W.E., Eckert, G.P., 2008. Isoprenoid quantitation in human brain tissue: a validated HPLC-fluorescence detection method for endogenous farnesyl- (FPP) and geranylgeranyl pyrophosphate (GGPP). Anal Bioanal. Chem. 392, 673–680.

Hooff, G.P., Wood, W.G., Kim, J.H., Igbavboa, U., Ong, W.Y., Muller, W.E., Eckert, G.P., 2012. Brain isoprenoids farnesyl pyrophosphate and geranylgeranyl pyrophosphate are increased in aged mice. Mol. Neurobiol. 46, 179–185.

Hooff, G.P., Wood, W.G., Muller, W.E., Eckert, G.P., 2010. Isoprenoids, small GTPases and Alzheimer's disease. Biochim. Biophys. Acta 1801, 896–905.

Hottman, D.A., Li, L., 2014. Protein prenylation and synaptic plasticity: implications for Alzheimer's disease. Mol. Neurobiol. 50, 177–185.

Huesa, G., Baltrons, M.A., Gomez-Ramos, P., Moran, A., Garcia, A., Hidalgo, J., Frances, S., Santpere, G., Ferrer, I., Galea, E., 2010. Altered distribution of RhoA in Alzheimer's disease and AβPP overexpressing mice. J. Alzheimers Dis. 19, 37–56.

Jick, H., Zornberg, G.L., Jick, S.S., Seshadri, S., Drachman, D.A., 2000. Statins and the risk of dementia. Lancet 356, 1627–1631.

Khachaturian, Z.S., 1985. Diagnosis of Alzheimer's disease. Arch. Neurol. 42, 1097–1105.

Kho, Y., Kim, S.C., Jiang, C., Barma, D., Kwon, S.W., Cheng, J., Jaunbergs, J., Weinbaum, C., Tamanoi, F., Falck, J., Zhao, Y., 2004. A tagging-via-substrate technology for detection and proteomics of farnesylated proteins. Proc. Natl. Acad. Sci. U S A. 101, 12479–12484.

Kremer, A., Louis, J.V., Jaworski, T., Van, L.F., 2011. GSK3 and Alzheimer's disease: facts and fiction. Front Mol. Neurosci. 4, 17.

Lambert, J.C., Ibrahim-Verbaas, C.A., Harold, D., Naj, A.C., Sims, R., Bellenguez, C., DeStafano, A.L., Bis, J.C., Beecham, G.W., Grenier-Boley, B., Russo, G., Thorton-Wells, T.A., Jones, N., Smith, A.V., Chouraki, V., Thomas, C., Ikram, M.A., Zelenika, D., Vardarajan, B.N., Kamatani, Y., Lin, C.F., Gerrish, A., Schmidt, H., Kunkle, B., Dunstan, M.L., Ruiz, A., Bihoreau, M.T., Choi, S.H., Reitz, C., Pasquier, F., Cruchaga, C., Craig, D., Amin, N., Berr, C., Lopez, O.L., De Jager, P.L., Deramecourt, V., Johnston, J.A., Evans, D., Lovestone, S., Letenneur, L., Morón, F.J., Rubinsztein, D.C., Eiriksdottir, G., Sleegers, K., Goate, A.M., Fiévet, N., Huentelman, M.W., Gill, M., Brown, K., Kamboh, M.I., Keller, L., Barberger-Gateau, P., McGuiness, B., Larson, E.B., Green, R., Myers, A.J., Dufouil, C., Todd, S., Wallon, D., Love, S., Rogaeva, E., Gallacher, J., St George-Hyslop, P., Clarimon, J., Lleo, A., Bayer, A., Tsuang, D.W., Yu, L., Tsolaki, M., Bossù, P., Spalletta, G., Proitsi, P., Collinge, J., Sorbi, S., Sanchez-Garcia, F., Fox, N.C., Hardy, J., Deniz Naranjo, M.C., Bosco, P., Clarke, R., Brayne, C., Galimberti, D., Mancuso, M., Matthews, F., European Alzheimer's Disease Initiative (EADI) Genetic and Environmental Risk in Alzheimer's Disease Alzheimer's Disease Genetic Consortium Cohorts for Heart and Aging Research in Genomic Epidemiology, Moebus, S., Mecocci, P., Del Zompo, M., Maier, W., Hampel, H., Pilotto, A., Bullido, M., Panza, F., Caffarra, P., Nacmias, B., Gilbert, J.R., Mayhaus, M., Lannefelt, L., Hakonarson, H., Pichler, S., Carrasquillo, M.M., Ingelsson, M., Beekly, D., Alvarez, V., Zou, F., Valladares, O., Younkin, S.G., Coto, E., Hamilton-Nelson, K.L., Gu, W., Razquin, C., Pastor, P., Mateo, I., Owen, M.J., Faber, K.M., Jonsson, P.V., Combarros, O., O'Donovan, M.C., Cantwell, L.B., Soininen, H, Blacker, D., Mead, S., Mosley Jr., T.H., Bennett, D.A., Harris, T.B., Fratiglioni, L., Holmes, C., de Bruijn, R.F., Passmore, P., Montine, T.J., Bettens, K., Rotter, J.I., Brice, A., Morgan, K., Foroud, T.M., Kukull, W.A., Hannequin, D., Powell, J.F., Nalls, M.A., Ritchie, K., Lunetta, K.L., Kauwe, J.S., Boerwinkle, E., Riemenschneider, M., Boada, M., Hiltuenen, M., Martin, E.R., Schmidt, R., Rujescu, D., Wang, L.S., Dartigues, J.F., Mayeux, R., Tzourio, C., Hofman, A., Nöthen, M.M., Graff, C., Psaty, B.M., Jones, L., Haines, J.L., Holmans, P.A., Lathrop, M., Pericak-Vance, M.A., Launer, L.J., Farrer, L.A., van Duijn, C.M., Van Broeckhoven, C., Moskvina, V., Seshadri, S., Williams, J., Schellenberg, G.D., Amouyel, P., 2013. Meta-analysis of 74,046 individuals identifies 11 new susceptibility loci for Alzheimer's disease. Nat. Genet. 45, 1452–1458.

Leduc, V., Jasmin-Belanger, S., Poirier, J., 2010. APOE and cholesterol homeostasis in Alzheimer's disease. Trends Mol. Med. 16, 469–477.

Leduc, V., Theroux, L., Dea, D., Dufour, R., Poirier, J., 2016. Effects of rs3846662 variants on HMGCR mRNA and protein levels and on markers of Alzheimer's disease pathology. J. Mol. Neurosci. 58, 109–119.

Leduc, V., Theroux, L., Dea, D., Robitaille, Y., Poirier, J., 2009. Involvement of paraoxonase 1 genetic variants in Alzheimer's disease neuropathology. Eur. J. Neurosci. 30, 1823–1830.

Li, G., Larson, E.B., Sonnen, J.A., Shofer, J.B., Petrie, E.C., Schantz, A., Peskind, E.R., Raskind, M.A., Breitner, J.C., Montine, T.J., 2007. Statin therapy is associated with reduced neuropathologic changes of Alzheimer disease. Neurology 69, 878–885.

Liao, J.K., Laufs, U., 2005. Pleiotropic effects of statins. Annu. Rev. Pharmacol. Toxicol. 45, 89–118.

Mo, H., Yeganehjoo, H., Shah, A., Mo, W.K., Soelaiman, I.N., Shen, C.L., 2012. Mevalonate-suppressive dietary isoprenoids for bone health. J. Nutr. Biochem. 23, 1543–1551.

Mohamed, A., Smith, K., Posse de Chaves, E., 2015. In: Zerr, I. (Ed.), The mevalonate pathway in Alzheimer's disease - cholesterol and non-sterol isoprenoids,

Alzheimer's disease - challenges for the future. InTech. https://doi.org/10.5772/59904. Available from: http://www.intechopen.com/books/alzheimer-s-disease-challenges-for-the-future/the-mevalonate-pathway-in-alzheimer-s-disease-cholesterol-and-non-sterol-isoprenoids.

Nguyen, U.T., Guo, Z., Delon, C., Wu, Y., Deraeve, C., Franzel, B., Bon, R.S., Blankenfeldt, W., Goody, R.S., Waldmann, H., Wolters, D., Alexandrov, K., 2009. Analysis of the eukaryotic prenylome by isoprenoid affinity tagging. Nat. Chem. Biol. 5, 227–235.

Ohm, T.G., Treiber-Held, S., Distl, R., Glockner, F., Schonheit, B., Tamanai, M., Meske, V., 2003. Cholesterol and tau protein–findings in Alzheimer's and Niemann Pick C's disease. Pharmacopsychiatry 36 Suppl 2, S120–S126.

Ostrowski, S.M., Wilkinson, B.L., Golde, T.E., Landreth, G., 2007. Statins reduce amyloid-beta production through inhibition of protein isoprenylation. J. Biol. Chem. 282, 26832–26844.

Park, J., Matralis, A.N., Berghuis, A.M., Tsantrizos, Y.S., 2014. Human isoprenoid synthase enzymes as therapeutic targets. Front Chem. 2, 50.

Perez-Costas, E., Gandy, J.C., Melendez-Ferro, M., Roberts, R.C., Bijur, G.N., 2010. Light and electron microscopy study of glycogen synthase kinase-3 beta in the mouse brain. PLoS One 5, e8911.

Pfaffl, M.W., Tichopad, A., Prgomet, C., Neuvians, T.P., 2004. Determination of stable housekeeping genes, differentially regulated target genes and sample integrity: BestKeeper–Excel-based tool using pair-wise correlations. Biotechnol. Lett. 26, 509–515.

Poirier, J., Miron, J., Picard, C., Gormley, P., Theroux, L., Breitner, J., Dea, D., 2014. Apolipoprotein E and lipid homeostasis in the etiology and treatment of sporadic Alzheimer's disease. Neurobiol. Aging 35 Suppl 2, S3–S10.

Reitz, C., 2013. Dyslipidemia and the risk of Alzheimer's disease. Curr. Atheroscler. Rep. 15, 307.

Riekse, R.G., Li, G., Petrie, E.C., Leverenz, J.B., Vavrek, D., Vuletic, S., Albers, J.J., Montine, T.J., Lee, V.M., Lee, M., Seubert, P., Galasko, D., Schellenberg, G.D., Hazzard, W.R., Peskind, E.R., 2006. Effect of statins on Alzheimer's disease biomarkers in cerebrospinal fluid. J. Alzheimers Dis. 10, 399–406.

Roskoski Jr., R., 2003. Protein prenylation: a pivotal posttranslational process. Biochem. Biophys. Res. Commun. 303, 1–7.

Sano, M., Bell, K.L., Galasko, D., Galvin, J.E., Thomas, R.G., van Dyck, C.H., Aisen, P.S., 2011. A randomized, double-blind, placebo-controlled trial of simvastatin to treat Alzheimer disease. Neurology 77, 556–563.

Sato, R., 2009. SREBPs: protein interaction and SREBPs. FEBS J. 276, 622–627.

Sayas, C.L., Moreno-Flores, M.T., Avila, J., Wandosell, F., 1999. The neurite retraction induced by lysophosphatidic acid increases Alzheimer's disease-like tau phosphorylation. J. Biol. Chem. 274, 37046–37052.

Scheper, W., Hoozemans, J.J., Hoogenraad, C.C., Rozemuller, A.J., Eikelenboom, P., Baas, F., 2007. Rab6 is increased in Alzheimer's disease brain and correlates with endoplasmic reticulum stress. Neuropathol. Appl. Neurobiol. 33, 523–532.

Su Hyeon Lee, J.L., Won-Yong, L., Bong Chul, C., Man Ho, C., 2011. Electrospray-mass Spectrometric analysis of plasma pyrophosphates separated on a multi-modal liquid chromatographic column. Mass Spectrom. Lett. 2, 92–96.

Taira, K., Bujo, H., Hirayama, S., Yamazaki, H., Kanaki, T., Takahashi, K., Ishii, I., Miida, T., Schneider, W.J., Saito, Y., 2001. LR11, a mosaic LDL receptor family member, mediates the uptake of ApoE-rich lipoproteins in vitro. Arterioscler Thromb. Vasc. Biol. 21, 1501–1506.

Takashima, A., 2006. GSK-3 is essential in the pathogenesis of Alzheimer's disease. J. Alzheimers Dis. 9, 309–317.

Tong, H., Wiemer, A.J., Neighbors, J.D., Hohl, R.J., 2008. Quantitative determination of farnesyl and geranylgeranyl diphosphate levels in mammalian tissue. Anal Biochem. 378, 138–143.

Wang, P.L., Niidome, T., Akaike, A., Kihara, T., Sugimoto, H., 2009. Rac1 inhibition negatively regulates transcriptional activity of the amyloid precursor protein gene. J. Neurosci. Res. 87, 2105–2114.

Wiemer, A.J., Hohl, R.J., Wiemer, D.F., 2009. The intermediate enzymes of isoprenoid metabolism as anticancer targets. Anticancer Agents Med. Chem. 9, 526–542.

Wolozin, B., Wang, S.W., Li, N.C., Lee, A., Lee, T.A., Kazis, L.E., 2007. Simvastatin is associated with a reduced incidence of dementia and Parkinson's disease. BMC Med. 5, 20.

Wood, W.G., Li, L., Muller, W.E., Eckert, G.P., 2014. Cholesterol as a causative factor in Alzheimer's disease: a debatable hypothesis. J. Neurochem. 129, 559–572.